THE ASTROPHYSICAL JOURNAL, 166:543–557, 1971 June 15

FAR-ULTRAVIOLET INTERSTELLAR ABSORPTION IN ORION AND MONOCEROS

STEPHEN V. WEBER*
E. O. Hulburt Center for Space Research, Naval Research Laboratory, Washington, D.C.

RICHARD C. HENRY
E. O. Hulburt Center for Space Research, and Johns Hopkins University, Baltimore, Maryland

AND

GEORGE R. CARRUTHERS
E. O. Hulburt Center for Space Research
Received 1970 December 18; revised 1971 January 29

ABSTRACT

Eleven groups of hot stars and 206 individual such stars have been examined in the ultraviolet at 1500 Å. Ten exhibit strong ultraviolet reddening according to a law $E(m_{1500} - V) = 6.0\ E(B - V)$, and about fifteen more are weakly reddened in a manner not inconsistent with that law, which is similar to laws derived by others. Most supergiants are fainter in the ultraviolet (relative to the visible) compared with main-sequence stars of the same $B - V$ color, in agreement with previous work. There is a very weak and perhaps not significant tendency for giant stars also to be slightly dim. Two star groups appear to be reddened in an anomalous manner. One group of stars, and six single stars, all unreddened or only slightly reddened, are anomalously bright at 1500 Å by about 1.3 mag. The two anomalously reddened objects could actually be examples of this new ultraviolet-bright class of stars, reddened in accord with the same reddening law as the other stars.

I. INTRODUCTION

At 0204 MST on 1969 September 21, an Aerobee-150 rocket carried an ultraviolet-sensitive electronographic camera to 160 km above White Sands, New Mexico. Eighteen good-quality photographs in the wavelength range 1230–2100 Å were obtained of five regions in Orion and Monoceros. The effective wavelength of the present photographs is about 1500 Å. The five plates contained in this paper display these photographs. Specifically, we have Figure 1 (Plate 4): northern Orion (superposition of four 7-second exposures); Figure 2 (Plate 5): western Orion (three exposures); Figure 3 (Plate 6): Monoceros (eight exposures); Figure 4 (Plate 7): central Orion (four exposures); and Figure 5 (Plate 8): southeastern Orion (three exposures). (Some plates include exposures that are not of photometric quality.) The exposures making up Figure 5 were taken when the rocket was below 120 km, where Schumann-Runge absorption by molecular oxygen dims the ultraviolet images. These data were not used in the present paper. Figures 6–10 are identification charts for the stars contained in each field, and Figure 11 gives a general indication of the regions observed and provides information on the visible-light brightness of many of the stars.

Some of these data have been discussed qualitatively (Henry and Carruthers 1970*a*, *b*), to obtain information concerning the nature of the interstellar grains.

In subsequent sections we shall discuss the quantitative treatment of the present data and their interpretation. First, however, we will review very briefly the history of ultraviolet intensity measurements of the stars, and of the measurement of interstellar absorption at these wavelengths.

* Present address: 1939 Hall, Princeton University, Princeton, New Jersey.

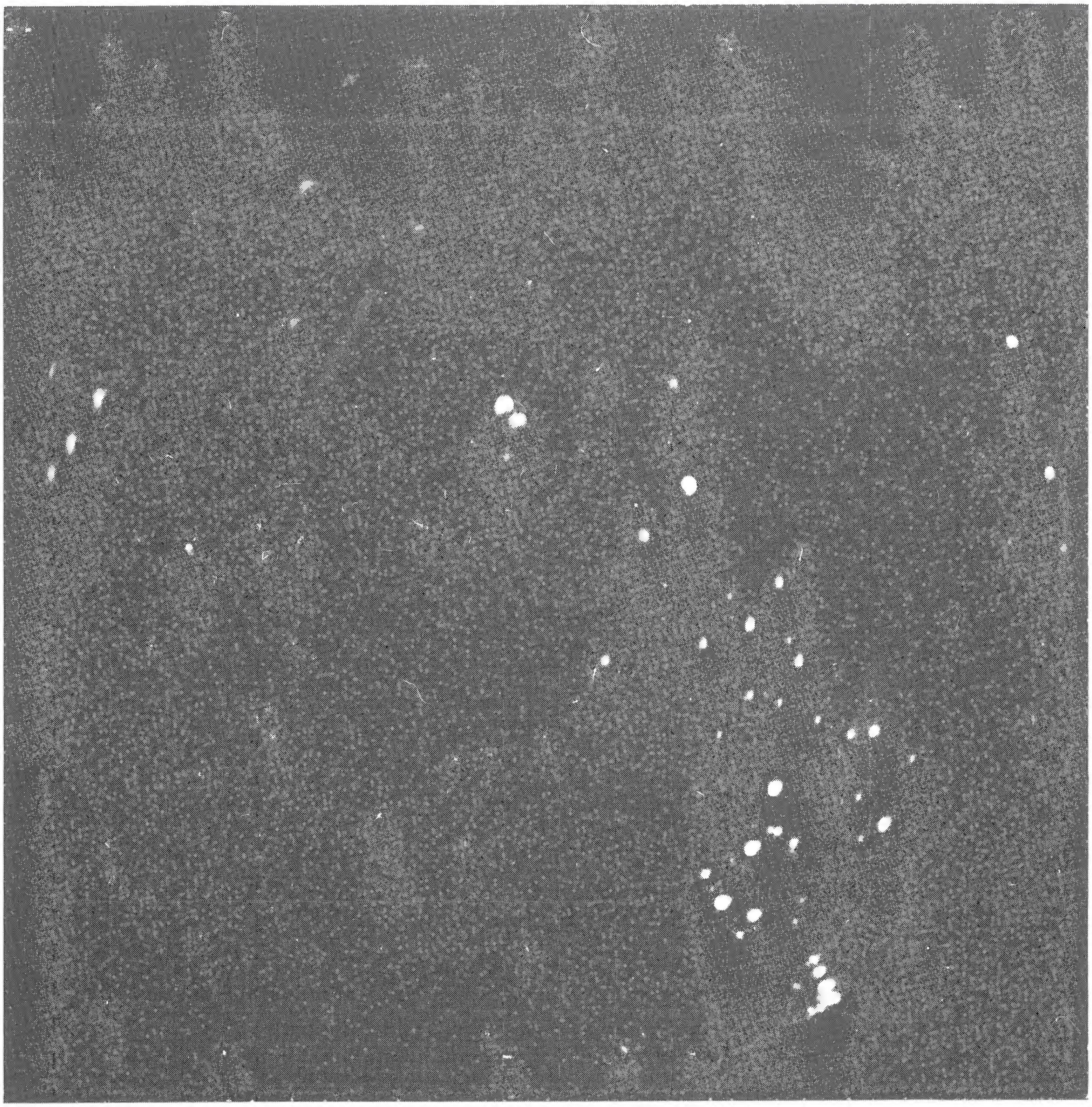

FIG. 1.—Far-ultraviolet (1500 Å) electronographic camera photograph of northern Orion. The diameter of the field of view is 25°. This is a superimposition of four 7-second exposures.

WEBER *et al.* (*see* page 543)

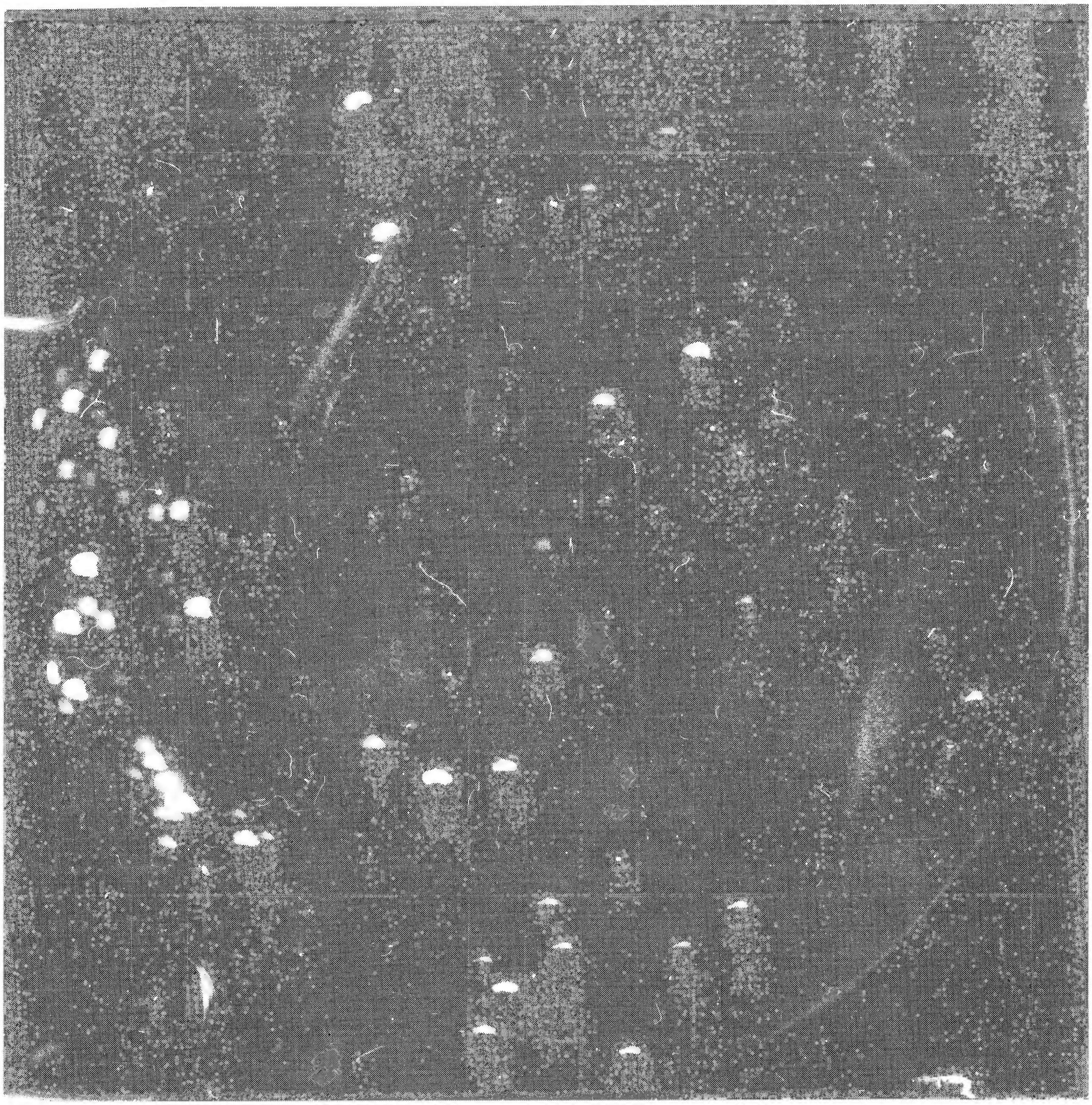

FIG. 2.—Western Orion (3 exposures)

WEBER et al. (see page 543)

FIG. 3.—Monoceros (8 exposures)

WEBER *et al.* (*see* page 543)

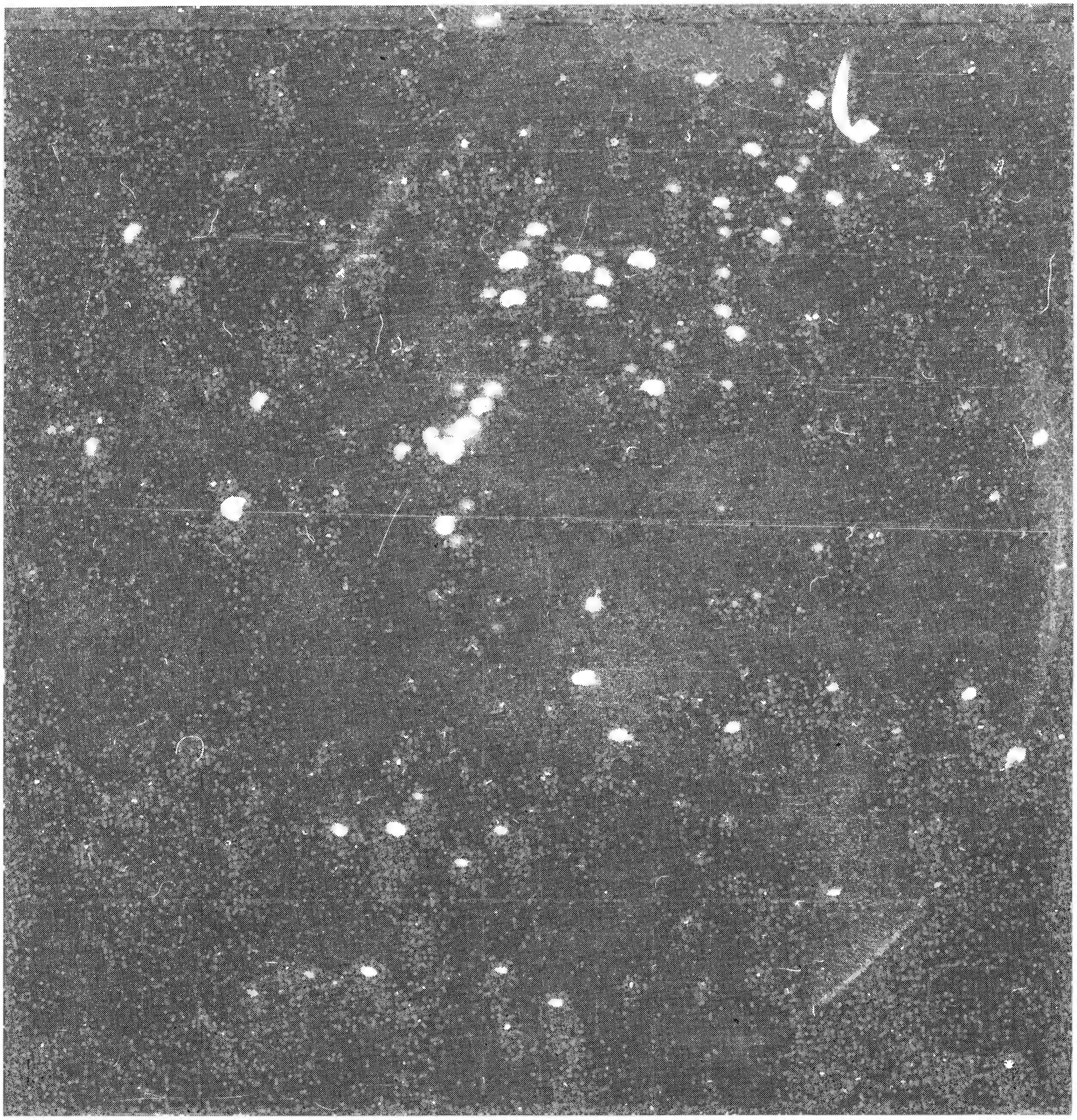

FIG. 4.—Central Orion (4 exposures)

WEBER *et al.* (*see* page 543)

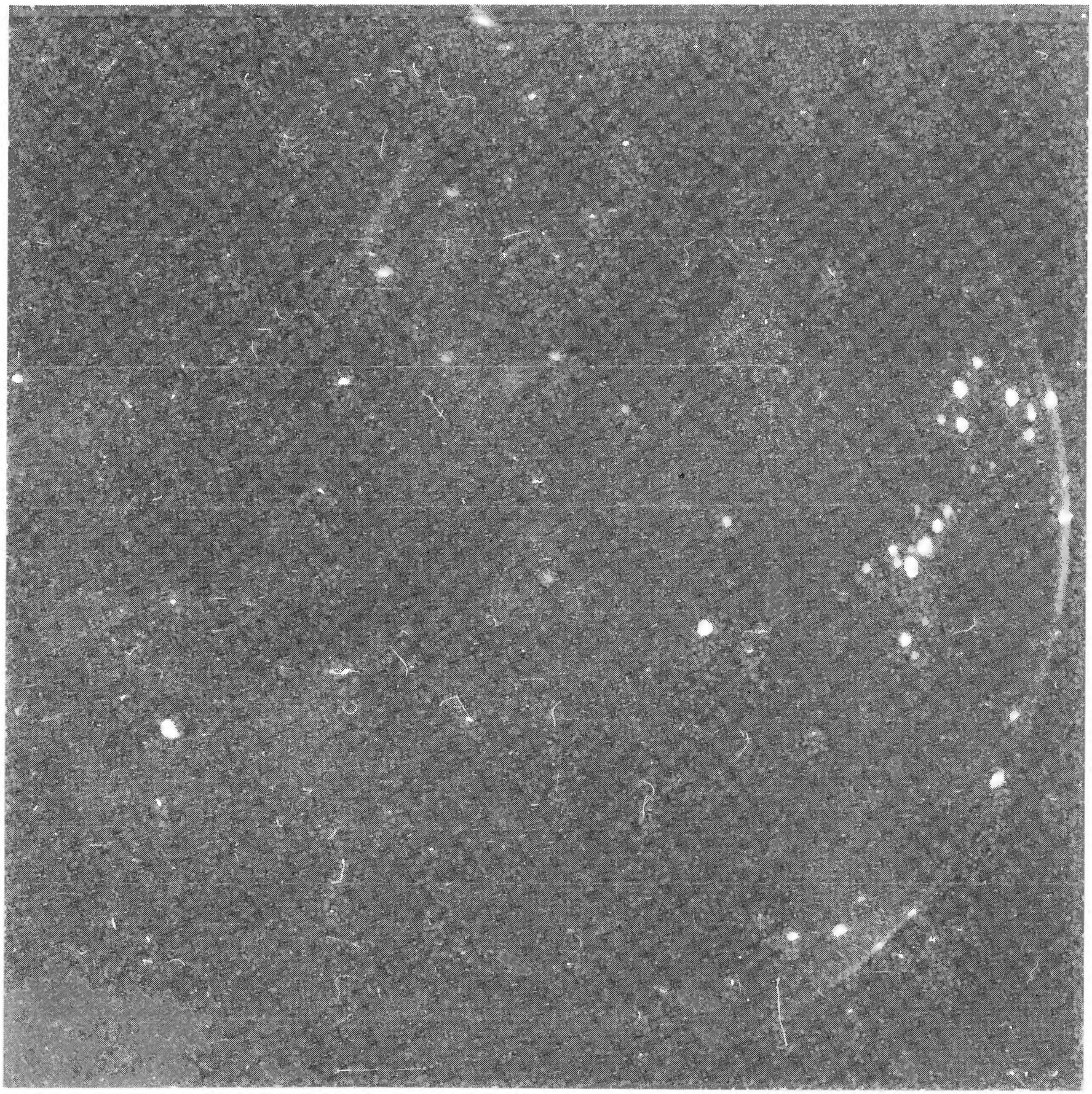

FIG. 5.—Southeastern Orion (3 exposures)

WEBER *et al.* (*see* page 543)

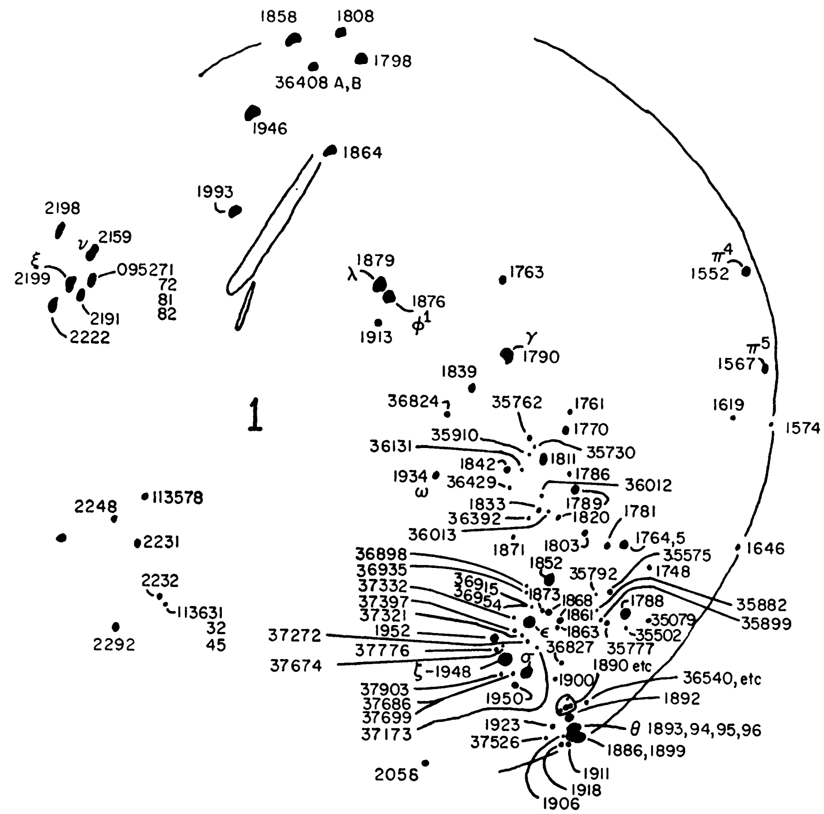

FIG. 6.—Identification chart for target 1 (Fig. 1). Numbers are Bright Star Catalog numbers or HD numbers.

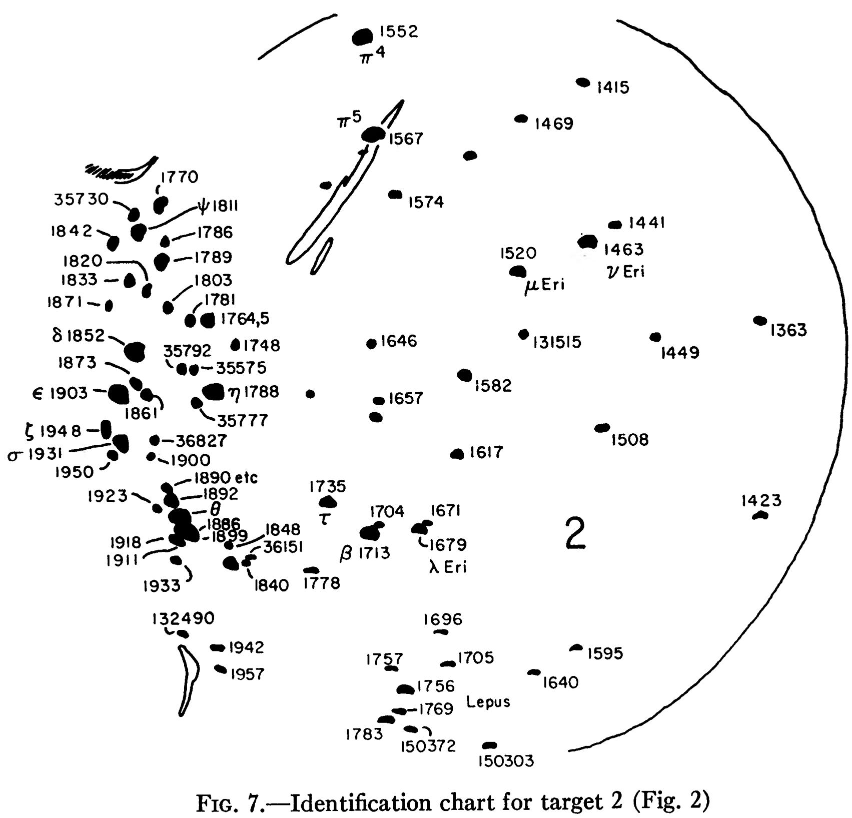

FIG. 7.—Identification chart for target 2 (Fig. 2)

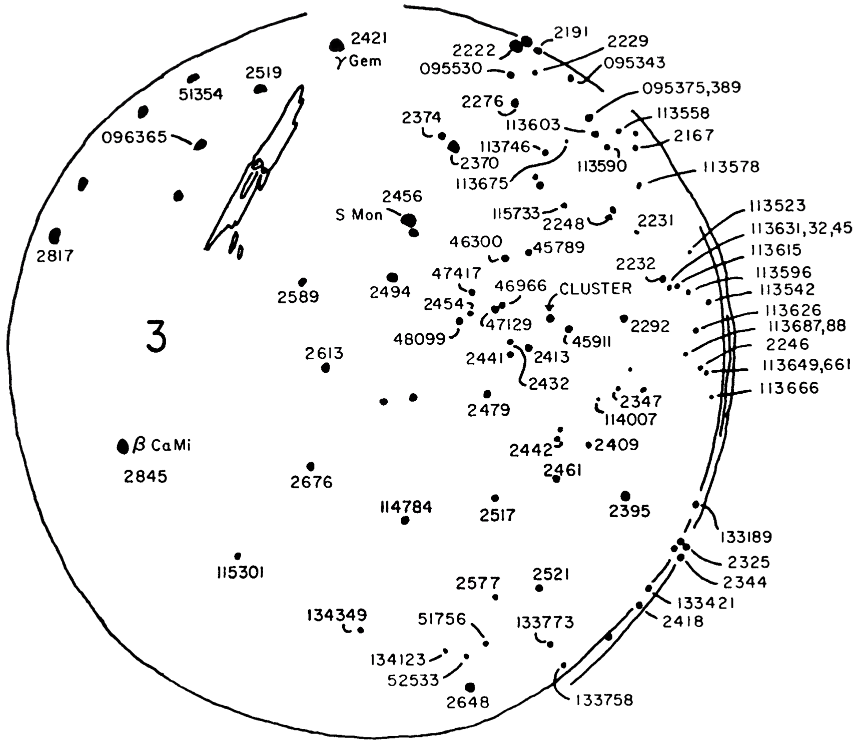

FIG. 8.—Identification chart for target 3 (Fig. 3)

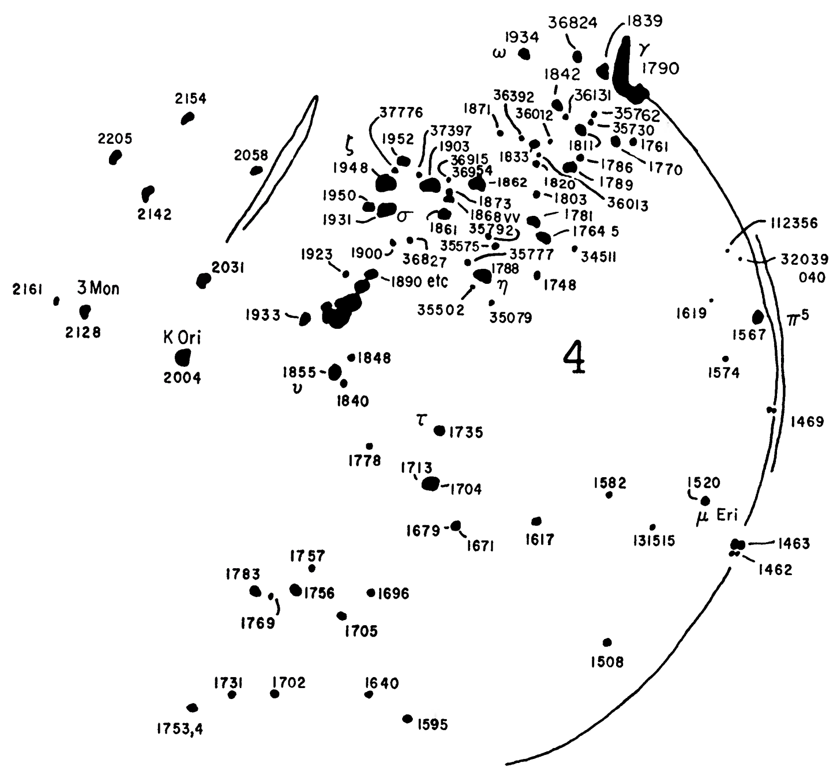

FIG. 9.—Identification chart for target 4 (Fig. 4)

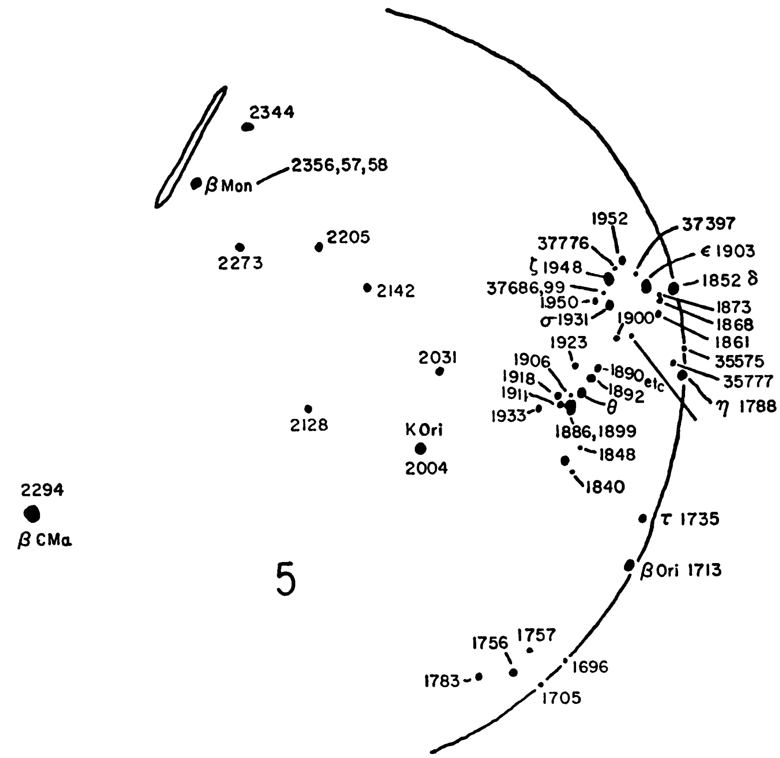

FIG. 10.—Identification chart for target 5 (Fig. 5)

The ultraviolet region of the spectrum was expected to be a rich source of information once space astronomy became practical, because it was known that O and B stars radiate most of their energy there. It was anticipated that theoretical models for these stars could be tested, that interstellar reddening could be investigated, and that observations of interstellar resonance lines would produce the best (or only) evidence regarding the interstellar abundance of common species such as oxygen. Actually, reliable upper limits on the oxygen abundance were first placed by means of X-ray astronomy (Rappaport, Bradt, and Mayer 1969; Fritz *et al.* 1971).

The investigation of interstellar reddening has produced an interesting result. Boggess and Borgman (1964) showed that the interstellar reddening in the far-ultraviolet is considerably greater than had been projected. The additional absorption is due to a previously unknown constituent of interstellar space. It may be dust particles $\sim 0.1\ \mu$ in size, or it might be a coating on the larger grains which has a low index of refraction. An important clue to the question of whether a truly independent source was responsible for the far-ultraviolet extinction apparently was provided when Carruthers (1969*a*) and Bless and Savage (1969) independently observed that the star θ Ori appears anomalously bright in the far-ultraviolet. Bless and Savage found the same to hold true for the star σ Sco. The interpretation was that the interstellar reddening curve was anomalous for these objects, in the sense that the second component, the far-ultraviolet absorbers, were absent or nearly so. We shall in the present paper show that there is reason to question this conclusion.

Finally, the history of the testing of models of early-type stars by observing the absolute brightnesses of actual stars in the far-ultraviolet appears to have been, so far, rather more of a venture in the study of ultraviolet calibration techniques than of

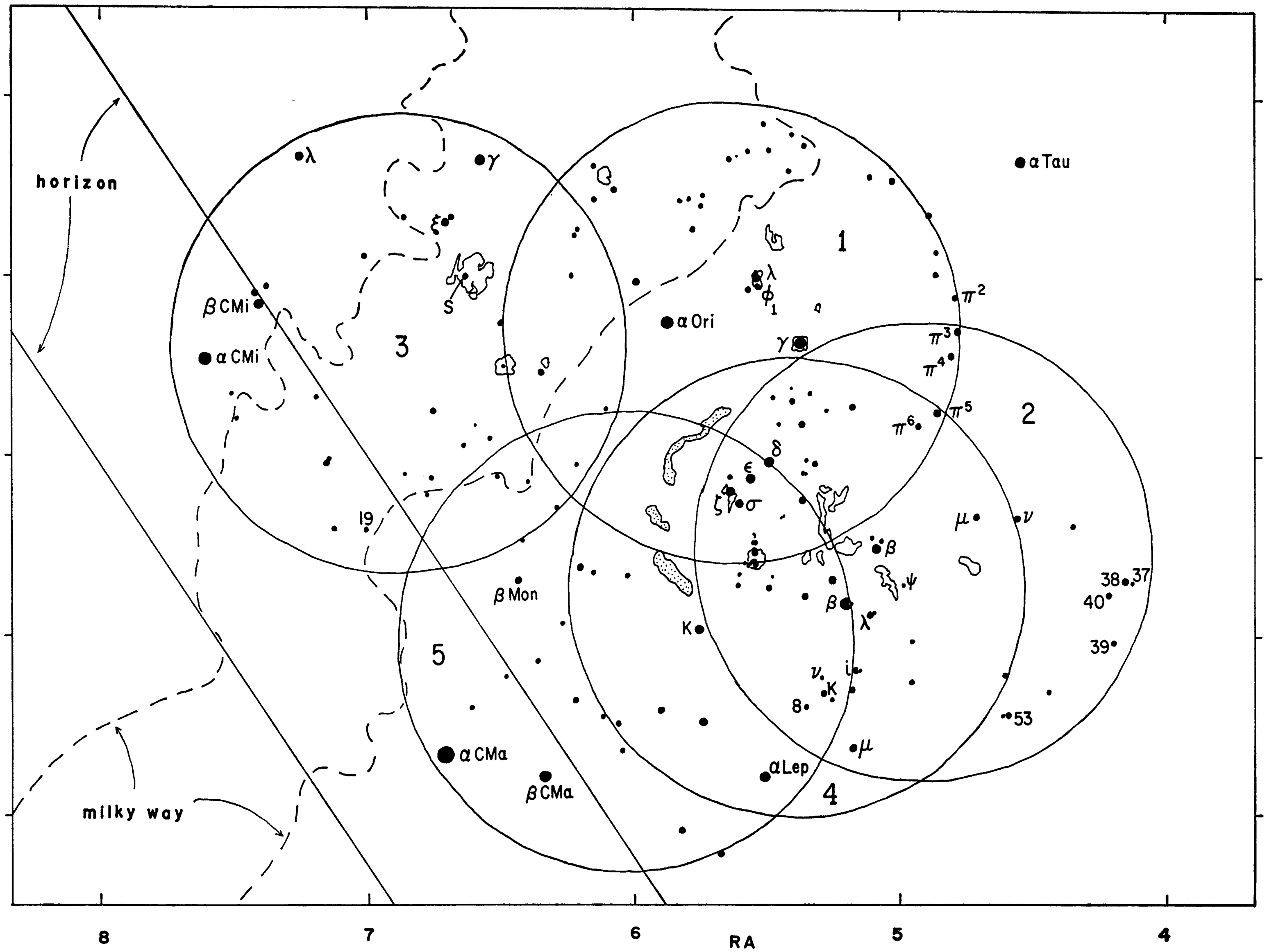

FIG. 11.—Map of the Orion-Monoceros region showing the five regions photographed (*circles*), and also the position of the horizon viewed from the ground and from maximum altitude. Star brightnesses are in the visible part of the spectrum. (Adapted from the *Atlas Coeli* [Becvar 1962].)

astronomy. In each wavelength interval, the first measurements indicated too low a brightness for the stars, and a scramble to find new sources of opacity in the appropriate wavelength range was precipitated. As calibration techniques improved, the stars gradually grew brighter and brighter, and interest in the opacity problem waned. Nonetheless, some recent measurements (Smith 1967; Opal *et al.* 1968) seem to indicate that at 1500 Å the B stars are 0.5 mag or more fainter than predicted by the models. Carruthers (1969*b*), however, finds quite good agreement between observations of stars in Orion and the line-blanketed models of Morton and his co-workers (e.g., Adams and Morton 1968).

II. REDUCTION OF DATA

Isodensitometry of our plates, in the manner of Kron, Ables, and Hewitt (1969), was not attempted owing to the large number and relatively poor quality of our data. Instead, the plates were measured with the Cuffey densitometer at Cerro Tololo Inter-American Observatory. This is a device in which a beam passes through a diaphragm centered on the star, and the diaphragm opening is adjusted so that the beam is of the same intensity as another beam which does not pass through the plates. The quantity $A_s - A_b$ is taken as an indicator of brightness, where A_s is the diaphragm area for the star image, and A_b the area for clear plate (but including sky fog).

Superpositions of from two to eight frames of target 3 were also measured, in an attempt to calibrate the data by assuming that a superposition of n plates was equivalent to n times the original exposure. This method, however, was found to underestimate the saturation by as much as several magnitudes for the brighter stars. Imperfect superposition of the images may be responsible for this effect. In the future, laboratory calibration will be done, and exposures of several different lengths will be taken to permit calibration. For the present plates no independent calibration curve could be used. This does not affect the use of the data to check the relative validity of stellar models, as will be seen. No absolute intensity calibration was attempted.

The raw brightnesses were found to vary systematically between the five targets. The photocathode of the camera was slightly tilted, and the resulting variation of focus across the field was considered responsible for this effect. A correction was applied, which gave agreement between targets within 0.25 mag. The targets had been chosen (Fig. 11) to be heavily overlapped to allow testing for this kind of effect. Results for images of the same star observed at different targets generally agree to within better than 0.1 mag. The residual differences between targets most likely result from variation in photocathode sensitivity, and different image shapes due to distortion in the system. Large systematic variations were present, however, between the frames of target 5. These frames were taken from below 120 km, so atmospheric absorption is responsible. Target 5 was not used in the analysis. Stars falling on the very edge of the field of view were also rejected.

Data on unresolved groups of stars observed in the present program are given in Table 1. Table 2 gives similar data on single stars, and Table 3 gives ultraviolet data for stars for which we could not locate adequate visible-light data.

The response functions of the electronographic camera (Henry and Carruthers 1970*b*) and of the V-filter were integrated with the B8 V, B9 V, and B9.5 V models of Mihalas (1966), O5 V and B0 V models of Hickok and Morton (1968), and main-sequence B stars from Van Citters and Morton (1970). For the ultraviolet, energy fluxes were converted to photon fluxes to which the electronographic camera is sensitive. It was thus determined that for main-sequence stars earlier than A0, $(m_{1500} - V) = 12.73\ (B - V)$ with $(m_{1500} - V)$ taken as 0 at $B - V = 0$. UBV photometry was found for most stars in the Naval Observatory catalog (Blanco *et al.* 1968) or in a few cases in Iriarte *et al.* (1965).

Theoretical magnitudes at 1500 Å were computed for all stars for which photometry was available, and in Figures 12 and 13 the theoretical magnitude is shown plotted

1971ApJ...166..543W

TABLE 1

Unresolved Groups of Stars

1	2	3	4	5	6	7	8	9	10	11
HR	HD	SP	V	B-V	E(B-V)	U-B	UV-V	E(UV)	NT	NF
1753	34798	B 5 V	6.36	-0.15	0.01	-0.59				
1754	34799	A 0 P	6.55	-0.11	0.01	-0.44				
			5.70		0.01		-0.66	0.18	1	4
1764	35007	B 3 IV	5.67	-0.13	0.06	-0.66				
1765	35039	B 2 IV	4.72	-0.17	0.06	-0.80				
			4.55		0.06		-2.92	0.09	3	11
	36117	A 0	7.97	+0.10	0.12	+0.02				
	36139	A 0	6.39	-0.01	-0.02	+0.03				
			6.16		0.00		-1.08	-1.13	1	3
	36540	B 9	8.11	+0.05	0.23	-0.49				
	36559	B 9	8.81	-0.05	0.01	-0.22				
	36629	B 5 V	7.65	+0.02	0.25	-0.66				
	36671	B 9	8.66	+0.34	0.27	+0.05				
			6.71		0.25		-2.16	0.21	1	3
	36842	B 9	8.09	-0.11	0.04	-0.51				
	36865	B 9	7.40	-0.07	0.06	-0.43				
	36883	B 8	7.22	-0.08	0.06	-0.47				
	36936	B 8	7.52	-0.11	0.06	-0.58				
			6.01		0.06		-2.22	-0.34	1	3
	36915	B 9	8.02	-0.01	0.10	-0.35				
	36954	B 3 V	6.95	-0.10	0.08	-0.65				
			6.60		0.09		-2.13	-0.85	2	7
1890	37017	B 2 V	6.55	-0.14	0.15	-0.78				
1891	37016	B 3 V	6.23	-0.15	0.11	-0.67				
1898	37040	B 3 V	6.30	-0.15	0.11	-0.68				
			5.16		0.12		-2.91	0.52	3	9
	37020	B 0.5 V	6.73	+0.02	0.32	-0.88				
	37021	B 3	8.1							
θ Ori	37022	O 6 P	5.13	+0.04	0.37	-0.95				
	37023	O 9.5 V	6.70	+0.09	0.33	-0.65				
	37041	O 9.5 VP	5.07	-0.08	0.22	-0.94				
	37042	B 1 V	6.39	-0.09	0.20	-0.92				
			3.98		0.30		-3.45	0.45	3	10
	37330	B 9	7.40	-0.09	0.07	-0.56				
	37342	B 9	8.01	-0.13	0.03	-0.56				
			7.00		0.04		-1.63	0.50	1	3
	37370AB	B 9	7.46	-0.04	0.10	-0.44				
	37370CD	B 9	7.95	+0.10	0.18	-0.15				
	37371A	B 9	8.83	+0.05	0.11	-0.13				
	37371B	B 9	8.66	+0.14	0.19	-0.05				
			6.69		0.12		-1.04	0.34	1	2
	37686	B 9	9.23	0.02	0.06	-0.09				
	37699	B 5	7.62	-0.13	0.07	-0.69				
			7.40		0.07		-2.64	-0.28	1	3

KEY TO TABLE 1

Table 1 contains data on groups of stars with individual visible-light photometry that are not resolved by the wide-field camera. Information contained in the various columns is as follows: Column (1), HR: Bright Star Catalog (BSC) number (Hoffleit 1964). Column (2), HD: Henry Draper number. Column (3), SP: MK spectral classification from Naval Observatory catalog (NOC), BSC, or Smithsonian catalog (1966). Column (4), *V*: *V*-magnitude from NOC or occasionally BSC. Column (5), $B-V$: $B-V$ color from NOC. Column (6), $E(B-V)$: color excess in $B-V$, calculated from $B-V$ and $U-V$. Column (7), $U-B$: $U-B$ color from NOC. Column (8), UV $-$ *V*: magnitude at 1500 Å minus *V*. Column (9), *E*(UV): color excess at 1500 Å. Column (10), NT: number of targets in which the star was measured. Column (11), NF: total number of frames on which the star was measured.

TABLE 2

Individual Unresolved Stars

1	2	3	4	5	6	7	8	9	10	11	12
N	HR	HD	SP	V	B-V	E(B-V)	U-B	UV-V	E(UV)	NT	NF
1	1312	26739	B 5 V	6.41	-0.11	0.04	-0.53	-2.17	-0.24	1	3
2	1363	27563	B 5 III	5.84	-0.14	-0.01	-0.50	-1.91	-0.20	1	3
3	1415	28375	B 8	5.54	-0.10	0.06	-0.54	-2.13	-0.13	1	3
4	1423	28497	B 1 V NE	5.59	-0.22	0.03	-0.89	-3.36	-0.24	1	3
5	1441	28843	B 9	5.80	-0.13	0.02	-0.55	-1.58	0.37	1	3
6	1449	29009	B 9	5.71	-0.14	-0.01	-0.48	-1.07	0.55	2	3
7	1463	29248	B 2 III	3.92	-0.21	0.10	-1.09	-2.78	1.17	2	3
8	1508	30076	B 2 V E	5.92	-0.11	0.14	-0.83	-2.61	0.59	2	7
9	1520	30211	B 5 IV *	4.02	-0.15	0.01	-0.60	-2.16	-0.07	2	7
10	1552	30836	B 2 III *	3.68	-0.17	0.06	-0.81	-2.17	0.76	2	7
11	1567	31237	B 2 III	3.73	-0.19	0.10	-1.01	-2.32	1.37	3	11
12	1570	31295	A 0 V	4.65	0.08	0.07	0.09	1.24	1.10	1	1
13	1574	31331	B 5	5.98	-0.13	0.02	-0.55	-1.88	0.07	3	7
14	1582	31512	B 9	5.50	-0.13	0.02	-0.54	-2.01	-0.11	2	7
15	1595	31726	B 1 V	6.14	-0.22	0.00	(1.16)	-3.13	-0.33	2	7
16	1617	32249	B 2 V	4.79	-0.20	0.00	-0.73	-2.61	-0.11	2	7
17	1640	32612	B 3	6.40	-0.19	0.00	(1.20)	-2.83	-0.41	2	7
18	1646	32686	B 5	6.04	-0.12	0.03	-0.52	-1.57	0.28	2	3
19	1657	32964	B 9	5.10	-0.06	-0.02	-0.17	-0.46	0.08	2	7
20	1666	33111	A 3 III	2.78	0.13	0.13	0.10	2.42	2.40	1	4
21	1671	33224	B 8	5.76	-0.05	0.06	-0.35	-1.55	-0.21	2	4
22	1679	33328	B 2 IV	4.27	-0.20	0.05	-0.90	-2.59	0.64	2	6
23	1690	33647	B 8 V *	6.67	-0.07	0.02	-0.33	0.30	1.50	1	3
24	1696	33802	B 8 V	4.46	-0.10	0.01	-0.40	-1.39	0.01	2	7
25	1702	33904	A P	3.30	-0.11	-0.01	-0.38	-0.73	0.54	1	4
26	1704	33948	A 0	6.36	-0.14	0.00	-0.53	-2.43	-0.60	2	4
27	1705	33949	B 8 V	4.36	-0.10	0.00	-0.37	-1.14	0.13	2	7
28	1713	34085	B 8 IA	0.08	-0.03	0.19	-0.69	0.78	3.63	2	6
29	1731	34447	B 3	6.56	-0.16	0.01	(1.24)	-2.55	-0.39	1	4
30	1735	34503	B 5 III	3.58	-0.12	0.01	-0.48	-1.59	0.08	2	7

TABLE 2 CONT.

1	2	3	4	5	6	7	8	9	10	11	12
N	HR	HD	SP	V	B-V	E(B-V)	U-B	UV-V	E(UV)	NT	NF
31		34511	B 5 V *	7.39	-0.10	0.11	-0.69	-2.38	0.25	2	8
32	1748	34748	B 1.5 V	6.32	-0.10	0.13	-0.75	-2.47	0.42	3	11
33	1756	34816	B 0.5 IV	4.29	-0.28	-0.01	-1.01	-2.70	0.75	2	7
34	1757	34863	B 7 V NN	5.29	-0.14	-0.03	(1.32)	-1.41	-0.01	2	7
35	1761	34959	B 5 P	6.51	-0.11	0.04	-0.52	-2.28	-0.39	2	7
36	1763	34989	B 1 V *	5.78	-0.12	0.15	-0.88	-3.10	0.28	1	4
37		35079	B 3 V *	7.07	-0.04	0.13	-0.54	-2.11	0.07	2	7
38	1769	35104	B 8	6.52	-0.09	0.04	-0.46	-1.16	0.53	2	7
39	1770	35149	B 1 V	5.00	-0.15	0.09	-0.82	-2.89	0.14	3	11
40	1778	35281	B 8	5.99	-0.04	0.07	-0.36	-1.25	0.16	2	6
41	1781	35299	B 2 V *	5.70	-0.22	0.02	-0.88	-3.31	-0.24	3	11
42	1783	35337	B 2 IV	5.24	-0.22	0.00	(1.16)	-2.93	-0.13	2	7
43	1786	35407	B 5 V *	6.31	-0.16	0.01	-0.62	-2.29	-0.13	3	11
44	1788	35411	B 0.5 V	3.32	-0.18	0.15	-1.10	-3.25	0.95	3	11
45	1789	35439	B 1 V PE	4.94	-0.21	0.04	-0.91	-3.12	0.12	3	11
46	1790	35468	B 2 III *	1.64	-0.23	0.01	-0.87	-1.15	1.86	1	4
47		35502	B 5 V *	7.36	-0.04	0.13	-0.54	-2.80	-0.62	1	4
48		35575	B 3 V *	6.43	-0.17	0.03	-0.73	-2.72	-0.13	3	3
49	1803	35588	B 3 V *	6.15	-0.18	0.03	-0.75	-2.73	-0.08	3	11
50	1808	35671	B 5 V	5.40	-0.10	0.06	-0.54	-1.89	0.11	1	4
51	1811	35715	B 2 IV *	4.59	-0.22	0.04	-0.92	-3.21	0.04	3	11
52		35730	B 5 V P *	7.20	-0.15	0.04	-0.69	-2.83	-0.34	3	10
53		35762	B 2 V *	6.74	-0.18	0.02	-0.73	-2.84	-0.28	2	7
54		35777	B 2 V *	6.61	-0.18	0.03	-0.75	-2.75	-0.10	3	11
55		35792	B 3 V *	7.21	-0.15	0.03	-0.65	-2.41	-0.10	3	9
56		35882	B 8 V *	7.78	-0.07	0.07	-0.48	-3.28	-1.45	1	3
57		35899	B 5 V *	7.53	-0.14	0.04	-0.63	-3.25	-0.99	1	3
58		35910	B 6 V *	7.58	-0.10	0.06	-0.55	-1.60	0.44	2	7
59	1820	35912	B 2 V *	6.37	-0.18	0.02	-0.74	-2.72	-0.12	3	11
60		36012	B 3	7.24	-0.10	0.09	-0.65	-1.56	0.91	2	6

TABLE 2 CONT.

1	2	3	4	5	6	7	8	9	10	11	12
N	HR	HD	SP	V	B−V	E(B−V)	U−B	UV−V	E(UV)	NT	NF
61		36013	B 5 V *	6.90	−0.15	0.03	−0.65	−2.36	−0.05	2	7
62		36133	B 2 V	6.94	−0.09	0.09	−0.60	−2.10	0.18	2	7
63		36151	B 5 V *	6.71	−0.13	0.03	−0.57	−2.18	−0.15	1	3
64	1833	36166	B 1.5 IV*	5.77	−0.20	0.03	−0.84	−3.14	−0.17	3	11
65	1839	36267	B 5 IV	4.20	−0.14	0.01	−0.54	−2.10	−0.23	2	7
66	1840	36285	B 1.5 V *	6.32	−0.19	0.04	−0.83	−3.03	−0.08	2	7
67	1842	36351	B 1.5 V	5.44	−0.19	0.04	−0.83	−3.09	−0.14	3	11
68		36392	B 3 V *	7.56	−0.14	0.05	−0.67	−2.19	0.24	2	7
69		36429	B 5 V *	7.56	−0.13	0.05	−0.64	−2.36	−0.03	1	3
70	1848	36430	B 2 V *	6.22	−0.17	0.04	−0.74	−2.70	−0.07	2	7
71	1852	36486	O 9.5 II	2.21	−0.21	0.16	−1.27	−1.69	3.02	3	11
72	1855	36512	B 0 V *	4.62	−0.26	0.04	−1.07	−3.40	0.37	2	7
73	1861	36591	B 1 V *	5.35	−0.20	0.07	−0.94	−3.29	0.11	3	10
74		36627	B 6 V *	7.56	−0.11	0.04	−0.54	−1.98	−0.02	1	1
75	1863	36646	B 3 V	6.52	−0.10	0.08	−0.62	−2.39	−0.05	1	3
76	1868	36695	B 1 V	5.35	−0.19	0.13	−1.09	−3.00	1.07	2	7
77	1871	36741	B 2 IV *	6.58	−0.20	0.01	−0.77	−2.82	−0.15	3	11
78	1873	36779	B 3 V *	6.23	−0.18	0.05	−0.81	−3.73	−0.83	3	8
79	1876	36822	B 0 IV	4.41	−0.17	0.11	−0.95	−3.22	0.31	1	4
80		36824	B 3 V *	6.69	−0.15	0.06	−0.72	−2.25	0.36	2	4
81		36827	B 5	6.69	−0.17	0.04	−0.74	−1.65	−0.01	3	11
82	1879	36861	O 8	3.39	−0.19	0.11	−1.02	−2.66	1.11	1	4
83		36898	B 5	7.04	−0.07	0.06	−0.43	−2.07	−0.45	1	3
84		36916	B 9	6.73	−0.10	0.07	−0.58	−2.35	−0.19	1	3
85		36935	B 8	7.52	−0.13	0.03	−0.56	−2.22	−0.23	1	1
86	1892	37018	B 2 V *	4.59	−0.20	0.06	−0.93	−3.47	−0.12	3	11
87	1900	37055	B 3 V *	6.40	−0.13	0.05	−0.63	−2.39	−0.11	3	11
88	1903	37128	B 0 IA *	1.70	−0.19	0.11	−1.04	−1.19	2.66	3	11
89		37129	B 2 V P *	7.13	−0.14	0.07	−0.73	−3.10	−0.41	1	2
90	1906	37150	B 3 V	6.54	−0.19	0.04	−0.81	−3.25	−0.38	3	4

TABLE 2 CONT.

1	2	3	4	5	6	7	8	9	10	11	12
N	HR	HD	SP	V	B−V	E(B−V)	U−B	UV−V	E(UV)	NT	NF
91		37173	B 8	7.86	−0.06	0.11	−0.55	−2.08	0.08	1	3
92	1911	37209	B 1 V *	5.70	−0.24	0.01	−0.91	−3.21	−0.07	3	4
93	1913	37232	B 1.5 V	6.10	−0.18	0.06	−0.84	−2.87	0.16	1	4
94		37272	B 9	7.91	−0.11	0.05	−0.56	−2.62	−0.57	1	3
95	1918	37303	B 1 V	6.03	−0.23	0.03	−0.93	−3.27	−0.01	3	5
96		37321	B 3 V *	7.10	−0.09	0.07	−0.55	−2.46	−0.39	1	3
97		37332	B 8	7.61	−0.13	0.04	−0.60	−2.50	−0.34	1	3
98		37397	B 3 V *	6.84	−0.16	0.05	−0.74	−2.42	0.25	2	7
99	1931	37468	O 9.5 V *	3.73	−0.24	0.05	−1.04	−2.76	0.98	3	11
100	1933	37481	B 1 V *	5.96	−0.23	0.02	−0.92	−3.28	−0.06	2	7
101	1934	37490	B 3 IIIE	4.54	−0.10	0.14	−0.80	−2.28	0.82	2	8
102		37526	B 3 V *	7.61	−0.12	0.04	−0.56	−2.86	−0.84	1	3
103	1942	37635	B 5	6.48	−0.11	0.02	−0.46	−1.98	−0.36	1	3
104		37674	B 8	7.67	−0.08	0.11	−0.63	−2.72	−0.28	2	3
105	1946	37711	B 3 IV	4.84	−0.13	0.05	−0.63	−2.19	0.10	1	4
106	1948	37742	O 9.5 IA*	1.75	−0.21	0.09	−1.06	−1.33	2.54	3	8
107	1950	37744	B 1 V *	6.21	−0.22	0.03	−0.90	−3.13	0.03	3	8
108	1952	37756	B 3 III *	4.93	−0.22	0.01	−0.84	−2.81	0.10	2	8
109		37776	B 2 V *	6.98	−0.15	0.10	−0.86	−2.93	0.28	2	4
110	1957	37808	B 8	6.36	−0.16	−0.02	−0.53	−1.52	0.25	1	3
111		37903	B 1.5 V	7.82	0.10	0.33	−0.62	−2.86	0.10	1	3
112	1923	38622	B 2 V *	5.27	−0.16	0.03	−0.67	−2.20	0.17	1	11
113	2004	38771	B 0.5 IB*	2.06	−0.18	0.12	−1.03	−1.35	2.50	1	4
114	2031	39291	B 2 V *	5.34	−0.20	0.03	−0.84	−2.81	0.16	1	3
115	2058	39777	B 2 V	6.55	−0.19	0.04	−0.81	−2.67	0.20	2	7
116	2128	40967	B 5 IV	4.95	−0.11	0.06	−0.60	−2.06	0.16	1	4
117	2142	41335	B 2 IV−V	5.22	−0.07	0.20	−0.85	−2.07	1.34	1	4
118	2154	41692	B 5 IV	5.37	−0.14	0.00	−0.53	−1.54	0.29	1	4
119	2159	41753	B 3 V *	4.41	−0.16	0.03	−0.67	−2.30	0.06	1	4
120	2161	41814	B 5	6.65	−0.16	0.02	(1.22)	−2.15	0.14	1	2

TABLE 2 CONT.

1	2	3	4	5	6	7	8	9	10	11	12
N	HR	HD	SP	V	B−V	E(B−V)	U−B	UV−V	E(UV)	NT	NF
121	2167	42035	B 9	6.54	−0.06	−0.01	−0.18	−0.38	0.20	1	8
122		42401	B 5	7.50	−0.03	0.15	(1.27)	−2.01	0.28	1	7
123	2199	42560	B 3 V *	4.47	−0.18	−0.01	−0.65	−2.22	0.00	2	4
124	2205	42690	B 3 IV *	5.04	−0.21	0.00	−0.77	−2.50	0.14	1	4
125	2222	43112	B 1 V	5.91	−0.23	0.04	−0.96	−3.30	0.09	2	4
126	2229	43247	B9II-III	5.33	−0.02	0.02	−0.13	0.10	0.59	1	8
127	2231	43285	B 5 E	6.05	−0.12	0.03	−0.54	−2.07	−0.13	2	10
128	2232	43317	B 5	6.63	−0.18	−0.01	−0.64	−2.66	−0.49	2	10
129	2246	43461	B 8	6.62	−0.05	0.09	−0.44	−1.23	0.49	1	7
130		43525	A 2 N	5.38	0.10	0.10	0.08	0.31	0.27	1	8
131	2248	43526	B 8	6.56	−0.10	0.05	−0.51	−1.89	−0.02	2	8
132	2292	44700	B 3 IV	6.40	−0.16	0.01	−0.62	−2.36	−0.21	2	10
133		45314	OE 9 PE	6.63	0.16	0.49	−0.88	−1.66	2.59	1	8
134		45786	B 3	7.09	−0.13	0.04	(1.25)	−2.23	−0.07	1	7
135		45911	B 2 V	7.31	−0.14	0.02	(1.25)	−2.47	−0.43	1	9
136	2370	45995	B 2 V	6.14	−0.07	0.20	−0.86	−2.46	0.99	1	9
137	2374	46075	B 6 V	6.42	−0.13	−0.02	−0.42	−1.05	0.34	1	6
138		46300	A 0 IB	4.49	0.02	0.11	−0.26	0.85	2.02	1	8
139	2395	46487	B 6 V	5.09	−0.15	0.00	−0.56	−2.14	−0.21	1	9
140	2409	46769	B 8 IB	5.79	0.00	0.15	−0.46	−0.91	1.05	1	8
141	2413	46885	B 8 V	6.54	−0.06	0.02	−0.28	−0.57	0.44	1	9
142		46966	O 8	6.86	−0.04	0.26	−0.93	−2.21	1.63	1	9
143	2421	47105	A 0 V	1.93	0.00	−0.01	0.03	0.61	0.48	1	9
144		47129	O 8	6.06	0.05	0.36	−0.89	−2.15	1.80	1	9
145	2432	47240	B 1 IB	6.15	0.14	0.42	−0.75	−0.57	3.06	1	9
146		47417	B 0 IV	6.97	0.01	0.30	−0.86	−1.65	2.05	1	9
147	2441	47431	B 6 V	6.56	−0.07	0.03	−0.34	−1.54	−0.31	1	9
148	2454	47756	B 5 V	6.50	−0.14	−0.01	−0.49	−0.64	1.02	1	8
149	2456	47839	O 7	4.66	−0.25	0.05	−1.07	−3.51	0.29	1	8
150	2461	47964	B 8 III	5.78	−0.10	−0.01	−0.35	−1.12	0.06	1	9

TABLE 2 CONT.

1	2	3	4	5	6	7	8	9	10	11	12
N	HR	HD	SP	V	B−V	E(B−V)	U−B	UV−V	E(UV)	NT	NF
151		48099	O 6	6.37	−0.05	0.25	−0.94	−2.55	1.30	1	9
152	2479	48434	B 0 III	5.89	−0.02	0.28	−0.90	−1.82	1.96	1	1
153	2494	48977	B 3 V	5.92	−0.18	0.00	−0.68	−2.73	−0.38	1	9
154	2517	49567	B3II-III	6.14	−0.14	0.05	−0.67	−2.34	0.09	1	9
155	2519	49606	B 8 III	5.73	−0.13	0.01	−0.52	−1.31	0.50	1	8
156	2577	50820	B3 V + K	6.20	0.56	0.82	−0.36	−1.07	2.19	1	9
157	2589	51104	B 7 V	5.89	−0.07	0.03	−0.35	−1.32	−0.04	1	8
158		51354	B 3 E	7.12	−0.18	−0.01	−0.65	−2.34	−0.12	1	9
159		51756	B 0.5 IV	7.23	−0.07	0.22	−0.91	−2.60	1.07	1	8
160	2613	51892	B 8	6.34	−0.11	0.02	−0.47	−1.42	0.25	1	6
161		52533	B 3	7.69	−0.08	0.22	−0.95	−2.69	1.11	1	8
162	2648	52918	B 1 V	4.98	−0.20	0.06	−0.93	−2.39	0.97	1	9
163	2676	53929	B 8	6.10	−0.13	0.00	−0.48	−1.69	−0.04	1	8
164	2817	58050	B 3 III	6.34	−0.13	0.15	−0.93	−2.72	0.84	1	7
165	2840	58599	B 6 IV	6.29	−0.13	0.00	−0.47	−1.15	0.46	1	2
166	2845	58715	B 8 V	2.89	−0.10	−0.02	−0.30	−0.70	0.28	1	9

KEY TO TABLE 2

Table 2 contains data on single stars for which visible-light photometric data were available. Information contained in the various columns is as follows: Column (1), N: A consecutive number used in this study. Columns (2) and (3), HR and HD: Same as cols. (1) and (2) of Table 1. Column (4), SP: Same as col. (3) of Table 1, except that an asterisk indicates that the luminosity class has been checked by using sources cited in the text. Columns (5), (6), and (7), V, $B - V$, $E(B - V)$: Same as cols. (4), (5), and (6) of Table 1. Column (8), $U - B$: Same as col. (7) of Table 1, except that a value in parentheses is on the Cape refractor system. Columns (9)–(12), UV $- V$; E(UV), NT, NF: Same as cols. (8)–(11) of Table 1.

TABLE 3

ULTRAVIOLET DATA ON STARS FOR WHICH *UBV* PHOTOMETRY WAS NOT AVAILABLE

1	2	3	4	5	6	7
N	NAME	SP	V	UV	NT	NF
167	HR 1469	B 7 V	5.30	3.60	2	3
168	HR 1798	B 3 N	6.16	4.18	1	3
169	HR 1858	B P	5.54	3.79	1	3
170	HR 1864	B 3	5.54	3.27	1	4
171	HR 2276	B 5 N	6.40	5.22	1	8
172	HR 2442	O 9.5 II	6.14	5.34	1	9
173	CLUSTER			4.14	1	8
174	095441	B 8	8.3	7.87	1	1
175	095530	B 9	8.2	5.35	1	9
176	095567	B 5	7.29	5.74	1	9
177	096365	B 8	6.69	5.12	1	5
178	112356	B 9	7.6	5.83	3	9
179	112364	B 8	8.3	7.16	1	2
180	113167	B 8	8.0	6.79	1	3
181	113523	B 8	8.4	6.59	1	6
182	113542	B 9	6.9	5.84	1	8
183	113558	B	8.6	5.92	3	7
184	113578	B 2	6.9	4.91	2	9
185	113590	B 9	8.2	6.61	1	1
186	113596	B 8	7.9	6.06	1	8
187	113603	B 8	8.0	6.30	1	7
188	113615	B 9	7.9	6.63	1	7
189	113626	B 9	7.6	5.76	1	8
190	113666	B 8	7.6	6.41	1	7
191	113746	B 8	8.3	6.16	1	7
192	114204	B 5	8.2	6.20	1	6
193	114762	B 8	6.60	5.07	1	8
194	115301	B 5	6.84	4.67	1	8
195	131515	B 8	7.5	5.06	2	6
196	131766	B 9	8.0	4.31	1	4
197	131889	B 8	7.7	5.18	2	8
198	132490	B 9	7.8	5.16	1	3
199	133148	B 9	8.0	7.04	1	9
200	133215	B 8	6.56	5.84	1	8
201	133758	B 8	6.64	4.27	1	7
202	133773	B 8	8.0	4.88	1	8
203	134123	B 8	8.3	5.81	1	9
204	134349	B 9	8.8	4.95	1	9
205	150303	B 8	6.74	2.27	1	3
206	150372	B 8	7.1	5.39	1	3

KEY TO TABLE 3

Table 3 contains data on stars for which *UBV* photometry was not located. Information contained in the various columns is as follows: Column (1), N: Consecutive number continued from Table 2. Column (2), Name: Number in Smithsonian catalog unless otherwise noted. Cluster is NGC. Column (3), SP: MK spectral classification for bright stars from BSC; others are from Smithsonian catalog. Column (4), *V:* Visual magnitude; same sources as for col. (3). Column (5), UV: Measured magnitude at 1500 Å. Columns (6) and (7), NT, NF; Same as cols. (10) and (11) of Table 1.

against the observed magnitude = (const.) $[-2.5 \log (A_s - A_b)]$, corrected for focus variations. Figure 12 contains only stars visually reddened 0.05 mag or less. The relation is nearly linear over most of the range of observation. Since no calibration was used, this linearity is not expected, and in fact would not have resulted if the electronographic system had had a linear response to incident photons. This is because the quantity $(A_s - A_b)$ is proportional to the total light absorbed from the densitometer beam, whereas the true stellar intensity would be proportional to the integral of density $d = \log (I_0/I)$ over the image (where I_0 and I are the initial and transmitted beam intensities, respectively). The intensity distribution in the images is determined largely by the chromatic aberration of the Schmidt corrector, and is strongly peaked near the centers

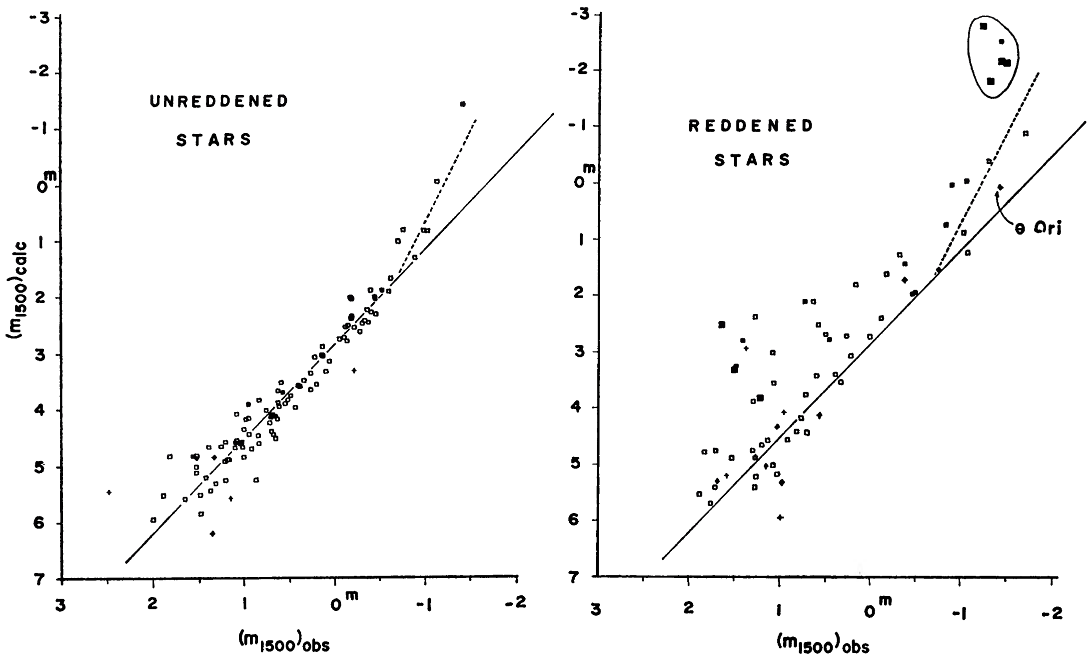

FIG. 12 FIG 13

FIG 12.—Magnitudes at 1500 Å as calculated from stellar models and as observed, for stars visually reddened 0.05 mag or less. A least-squares straight line is shown; *dashed line*, a suggested departure from this for the brightest stars. Only the scatter at a given magnitude is meaningful, as no ultraviolet calibration was available. *Filled squares*, giant stars. *Crosses*, stars for which some external reason exists for doubting the ultraviolet magnitude. *Diamonds*, groups of stars.

FIG. 13.—Similar to Fig. 12, but here only stars reddened more than 0.05 mag are plotted. *Solid* and *dashed lines*, same as Fig. 12. A group of giants and supergiants (*large filled squares*) has been isolated.

of the images. Therefore, a relationship between $(A_s - A_b)$ and intensity, in the absence of a set of images of known intensity ratio, could only be derived by detailed scanning of the images.

The least-squares line shown in Figure 12 was adopted for use as a calibration curve, although the poorly determined upper section of the curve may be above this line; the dotted line is one possibility. The scatter is seen to be fairly small, and is somewhat greater at the high and low ends of the curve.

III. DISCUSSION

The data of Figure 12 were used as a calibration curve. Investigation of departures from this calibration curve for reddened stars is carried out below. The data are usable in this way only because a very tight relation between observed and calculated magnitudes occurred for these unreddened stars. The scatter, if a very few individual stars are ignored, is about the same as the scatter between measurements of the same star on separate targets; that is, the scatter is within the error of observation.

The fact that this occurred (again if a few deviant stars are temporarily ignored) indicates that all stars of a given visible $(B - V)$ color have the same $(m_{1500} - V)$ color within about 0.5 mag. A possible minor exception to this statement occurs for the giant stars (*filled symbols* in Fig. 12), which may be slightly fainter than main-sequence stars (relative to the visible) at 1500 Å.

Also, differences that the models predict between the $(m_{1500} - V)$ colors of, say, B0 and B8 stars are correct, again to within about 0.50 mag, or a larger scatter would result in the diagram.

Figure 13 is analogous to Figure 12, but shows stars that are visually reddened 0.06 mag or more. Some of the stars, most of them rather weakly reddened ones, fall near the curve; but most fall to the left of it, that is, appear to be fainter than predicted by the models. The group of supergiants and one bright giant that would be most affected by choosing a higher calibration curve are circled in the figure.

Color excesses at 1500 Å were computed based on the calibration curve assumed, i.e., the curve for unreddened stars in Figure 12. These color excesses are not absolute, but are relative to the mean visually unreddened main-sequence stars. If unknown absorption exists for these stars, or if the model atmospheres are incorrect, then the values will be in error. Figure 14 plots the observed ultraviolet color excesses against $E(B - V)$, the visual indicator of reddening. The luminosity classes designated have, whenever possible, been based on absolute magnitudes from Bappu *et al.* (1962), Beer (1961, 1964), and Crawford (1958). In most cases, the luminosity data confirmed existing classification. HR 2577, with a computed visual reddening of 0.82 mag, falls off this graph. This star is known to have a composite spectrum, so the reddening value is probably in error. The upper line represents the main-sequence reddening line, $E(m_{1500} - V) = 6.0\ E(B - V) - 0.18$. It passes slightly below the origin, since the mean reddening of the stars on which the calibration curve was based is greater than zero. The slope is about 6, which is within experimental error of the value 6.6 which would be expected at 1500 Å from the results of Smith (1967) and Stecher (1965).

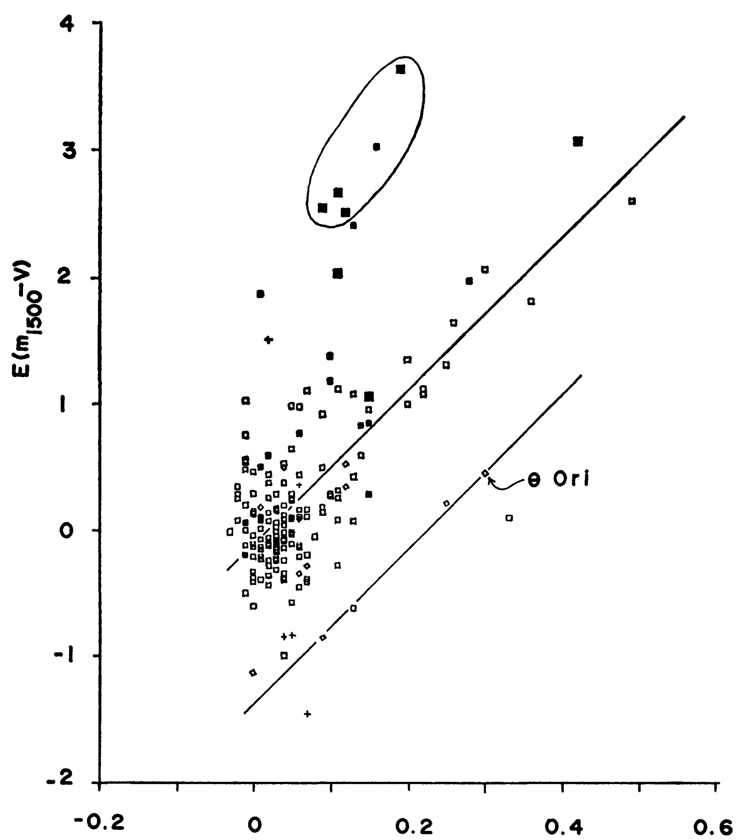

FIG. 14.—Excess $E(m_{1500} - V)$ is plotted against the $E(B - V)$. Upper straight line is a conventional ultraviolet-reddening law. A parallel line drawn through θ Ori also passes through a group of unreddened stars that appear to be 1.3 mag brighter than most main-sequence stars in the ultraviolet.

Supergiants all fall well above the main-sequence stars, except for HR 2409. No absolute magnitude was available for this star, and the luminosity classification should be checked. The circled group of supergiants HR 1713, HR 1903, HR 1948, and HR 2004 and the bright giant HR 1852 fall at the upper end of the calibration curve, and if that curve were adjusted as suggested by the dotted line, these stars would fall on points 1–2 mag fainter than the main sequence. Carruthers (1969*b*) has also found supergiants about 1 mag underluminous at 1115 Å, and Mihalas (1970) has shown that this effect is not inconsistent with theory. The giants HR 1790 and HR 1666 are also substantially fainter than main-sequence stars, and although absolute-magnitude data confirm the classification of HR 1790, these stars appear to share the ultraviolet deficiency of supergiants. HR 1690, marked with a cross, is very faint, and the observation is of doubtful validity.

There is a scattering of other stars that may be significantly above the main sequence in the figure—i.e., that may be faint at 1500 Å. Of these, HR 1788, HR 1879, and HR 1931 would be of expected brightness with adjustment of the calibration curve. Luminosity data are not available for the rest of these stars, and they may be giants. Most giants appear to be fainter than the average main-sequence star, although the error is too great to be certain of such an effect.

The most surprising anomalous objects are the stars which appear to be 1.3 mag overluminous. The star θ Ori has been observed previously by Carruthers (1969*a*), who found it 2 mag overluminous at 1115 and 1270 Å. His color excesses of 0.37 at 1115 Å and 0.53 at 1270 Å agree well with the excess of 0.45 we find at 1500 Å. The suggested adjustment of the calibration curve would reduce our value, but it would still agree to within the errors. The image of θ Ori appears to blend with that of HR 1892 and HR 1899 on the published plates, but on the original individual frames it is well separated, and the measurement should not be in error. Two new objects which exhibit strong visual reddening but apparently little in the ultraviolet are HD 37903 and the group consisting of HD 36540, HD 36559, HD 36629, and HD 36671. There appears to be no reason to reject HD 37903, but the group has a somewhat extended image which might have affected the measurement. Carruthers has suggested that reduced absorption is responsible for the brightness of θ Ori, and the same effect could be responsible for the other two objects.

There are, however, several visually unreddened or only slightly reddened stars which exhibit the same abnormal brightness at 1500 Å. A line parallel to the normal reddening line and passing through θ Ori gives a good fit to these stars. The observational data on these objects have been carefully checked. HD 35502, HD 35899, and the pair HD 36915 and 36954 appear to be perfectly acceptable. HD 35882 is in a region of relatively high plate fog, HD 37526 is not far from the edge of the field, and HR 1873 is rather close to a brighter star. The measurements for these stars could be in error, so they are plotted as crosses; however, they are probably valid points. The object listed as HD 36117 and HD 36139 has probably been misidentified, and is not plotted. All of these overluminous stars except θ Ori and HR 1873 are faint, which may make them subject to greater error. However, they seem to be significantly separated from the general scatter around zero reddening which includes many faint stars. All of these overluminous stars are main-sequence numbers of the I Ori association, so it is not unreasonable that few of them are bright.

There is considerable difficulty in accounting for the overluminous nature of these stars. Carruthers (1969*a*) found that if θ Ori followed the normal reddening law, it would have to be bluer than an infinite-temperature blackbody. Far-ultraviolet emission lines could produce some excess radiation, but it seems unlikely that factors of 2 or more could be accounted for in this way. In the case of θ Ori (Carruthers 1969*a*) there do not appear to be any strong emission lines in the 1000–1400 Å wavelength range. It may seem premature to deduce the existence of a class of intrinsically overluminous stars from data of the present quality. On the other hand, there is no reasonable cause to discount the visually unreddened and apparently overluminous stars found in this study, and further intensive investigations of these stars is urgently needed, both in the ground-accessible wavelength range and in the far-ultraviolet. In particular, data obtained by the instruments aboard the Orbiting Astronomical Observatory (OAO-A2) for stars in common with the present investigation should be studied, and ground-based photometry and spectra of these stars should be rechecked. It is possible that observed excess brightnesses could be due to errors in the visual colors and spectral classifications, to local anomalies in the interstellar-extinction law, or to both; and only more detailed investigations at all relevant wavelengths can resolve this question.

We are indebted to personnel of the White Sands Missile Range and the Aerojet-General Corporation, and to Dr. N. Paul Patterson, for their support of this rocket flight. Mr. Harry Merchant provided technical support for the experiment. One of us (R. C. H.) was supported in part by National Science Foundation grants GS-8313, 7086, and 11855. The instrument development was also partially supported by the NSF.

REFERENCES

Adams, T. F., and Morton, D. C. 1968, *Ap. J.*, **152**, 195.
Bappu, M. K. V., Chandra, S., Sanwal, N. B., and Sinvhal, S. D. 1962, *M.N.R.A.S.*, **123**, 521.
Becvar, A. 1962, *Atlas Coeli* (Cambridge, Mass.: Sky Publishing Co.).
Beer, A. 1961, *M.N.R.A.S.*, **123**, 191.
———. 1964, *ibid.*, **128**, 261.
Blanco, V. M., Demers, S., Douglass, G. G., and Fitzgerald, M. P. 1968, *Pub. U.S. Naval Obs.*, Series 2, Vol. **21**.
Bless, R. C., and Savage, B. D. 1969, *I.A.U. Symp. No. 36*.
Boggess, A., and Borgman, J. 1964, *Ap. J.*, **140**, 1636.
Carruthers, G. R. 1969*a*, *Ap. J.* (*Letters*), **147**, L113.
———. 1969*b*, *Ap. and Space Sci.*, **5**, 387.
Crawford, D. L. 1958, *Ap. J.*, **128**, 185.
Fritz, G., Henry, R. C., Meekins, J. F., Chubb, T. A., and Friedman, H. 1971, *Ap. J.* (in press).
Henize, K. G., Wackerling, L. R., and O'Callaghan, F. G. 1967, *Science*, **155**, 1407.
Henry, R. C., and Carruthers, G. R. 1970*a*, *Bull. A.A.S.*, **2**, 198.
———. 1970*b*, *Science*, **170**, 527.
Hickok, F. R., and Morton, D. C. 1968, *Ap. J.*, **152**, 203.
Hoffleit, D. 1964, *Yale Catalog of Bright Stars* (New Haven, Conn.: Yale University Observatory).
Iriarte, B., Johnson, H. L., Mitchell, R. I., and Wisnieski, W. K. 1965, *Sky and Tel.*, **30**, 21.
Kron, G. E., Ables, H. D., and Hewitt, A. V. 1969, in *Advances in Electronics and Electron Physics*, Vol. **28A**, ed. J. D. McGee *et al.* (New York: Academic Press), p. 1.
Mihalas, D. 1966, *Ap. J. Suppl.*, **13**, 1.
———. 1970, *Ap. and Space Sci.*, **8**, 50.
O'Dell, C. R., York, D. G., and Henize, K. G. 1967, *Ap. J.*, **150**, 835.
Opal, C. B., Moos, H. W., Bottema, M., Fastie, W. G., and Henry, R. C. 1968, *Ap. J.* (*Letters*), **153**, L179.
Rappaport, S., Bradt, H. V., and Mayer, W. 1969, *Ap. J.* (*Letters*), **157**, L21.
Smith, A. M. 1967, *Ap. J.*, **147**, 158.
Smithsonian Star Catalog. 1966 (Washington: Smithsonian Institution).
Stecher, T. P. 1965, *Ap. J.*, **142**, 1683.
Van Citters, G. Wayne, and Morton, D. C. 1970, *Ap. J.*, **161**, 615.